ATLAS NOTE

ATLAS-CONF-2011-115

August 2, 2011

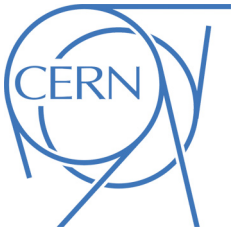

Search for heavy Majorana neutrino and W_R in dilepton plus jets events with the ATLAS detector in pp collisions at $\sqrt{s}$ = 7 TeV

The ATLAS Collaboration

Abstract

This note reports on a search for hypothetical heavy Majorana neutrinos and W_R gauge bosons in the context of the Left-Right Symmetric Model, in events with two isolated high-p_{T} same-sign or opposite-sign leptons and high-p_{T} hadronic jets. The data were collected with the ATLAS detector in proton-proton collisions at $\sqrt{s}$=7 TeV, at the CERN Large Hadron Collider (LHC), and correspond to an integrated luminosity of 34 pb^{-1}. No excess above the Standard Model background expectation is observed. Mass-dependent limits on the production cross-sections times branching ratio are presented for W_R gauge bosons masses below 1.8 TeV. The exclusion region is significantly larger than that obtained from previous measurements.

1 Introduction

The discovery [1] of large mixing between the second and the third generation in the neutrino sector of the Standard Model (SM) unambiguously established that neutrinos have non-zero masses and offers one of the most compelling indications of physics beyond the SM. A mass generation mechanism for the known neutrinos can be introduced with one or more additional neutrino fields, that could manifest themselves as new particles that could be directly observable at the LHC. The masses of the light neutrinos could be explained via the see-saw mechanism [2], which results in $m_\nu \approx m_D^2/M_N$, where for each generation, m_ν is the mass of a known light neutrino, m_D is the Dirac mass term for charged fermions of the same generation, and M_N is the mass of the new heavy neutrino. If the see-saw mechanism were to explain the masses of the known neutrinos, all would have to be Majorana particles. This would violate lepton number conservation, yielding a striking signature of two same-sign leptons.

This note reports on a search for heavy Majorana neutrinos, N, with data corresponding to an integrated luminosity of 34 pb^{-1}, recorded with the ATLAS detector. The approach is guided by the Left-Right Symmetric model (LRSM) in which a new gauge group with its force particles (W_R) manifesting themselves directly at LHC energies is introduced [3, 4]. In this model, the heavy neutrinos N are produced in the decays of a W_R via $q\bar{q} \to W_R \to lN$, with N decaying subsequently to $N \to lW_R^* \to ljj$. The final state signature is two high transverse momentum (p_{T}) leptons (electron or muon) and two high-p_{T} jets. The N and W_R invariant masses can be fully reconstructed from the decay products. Similarly to SM neutrinos, heavy Majorana neutrinos can mix if their masses are different. Both the scenarios of no-mixing and 100% mixing between two generations of lepton flavour (e or μ) are investigated.

Both the same-sign (SS) and opposite-sign (OS) dilepton final states are considered. If the heavy neutrinos are of Majorana type, they would contribute to both the SS and OS channels, while non-Majorana heavy neutrinos would contribute solely to the OS channel. The OS final state can be exploited for the LRSM search since the expected signal events, for the considered W_R masses, populate a kinematic region where the SM backgrounds are small.

Heavy neutrinos have been previously searched for at LEP [5, 6] and excluded for masses up to $\approx$ 100 GeV. The most stringent limits on the W_R bosons come from the Tevatron, which excluded W_R with masses below 739 GeV, if the W_R boson decays to either leptons or quarks [7].

Recently, ATLAS published an inclusive search for new physics in the same-sign dilepton signature [8] which presents limits on the LRSM up to W_R masses of about 1 TeV. This note complements the search presented in [8] and improves significantly the limits by performing an optimised search for LRSM signatures. The gain in sensitivity is achieved by additional selection criteria to improve the signal-to-background ratio, the use of the reconstructed W_R mass in setting the limit and the addition of the OS dilepton final state.

2 The ATLAS detector

The ATLAS detector [9] is a multipurpose particle physics apparatus with a forward-backward symmetric cylindrical geometry and a nearly 4π coverage in solid angle [1]. The inner tracking detector (ID) covers the pseudorapidity range $|\eta| < 2.5$, and consists of a silicon pixel detector, a silicon microstrip detector (SCT), and, for $|\eta| < 2.0$, a transition radiation tracker (TRT). The ID is surrounded by a thin superconducting solenoid providing a 2 T magnetic field. A high-granularity liquid-argon (LAr) sampling electromagnetic calorimeter covers the region $|\eta| < 3.2$. An iron-scintillator tile calorimeter provides

[1] ATLAS uses a right-handed coordinate system with its origin at the nominal interaction point (IP) in the centre of the detector and the z-axis coinciding with the axis of the beam pipe. The x-axis points from the IP to the centre of the LHC ring, and the y axis points upward. Cylindrical coordinates (r,ϕ) are used in the transverse plane, ϕ being the azimuthal angle around the beam pipe. The pseudorapidity is defined in terms of the polar angle θ as $\eta = -\ln\tan(\theta/2)$.

hadronic coverage in the central rapidity range of $|\eta| < 1.7$. The end-cap and forward regions, spanning $1.5 < |\eta| < 4.9$, are instrumented with LAr calorimeters for both electromagnetic and hadronic measurements. The muon spectrometer (MS) surrounds the calorimeters and consists of a system of air-core superconducting toroid coils, precision tracking chambers up to $|\eta| < 2.7$, and detectors for triggering in the region of $|\eta| < 2.4$.

3 Data and simulated events

The data used in this analysis were recorded in 2010 at the LHC at a centre-of-mass energy of 7 TeV. Application of beam, detector, and data-quality requirements results in a total integrated luminosity of 34 pb^{-1}, with an estimated uncertainty of 3.4% [10, 11]. The data were taken with single lepton (e or μ) triggers. At the last stage of the trigger decision, the electron trigger selects candidate electrons with transverse energy $E_{\text{T}} > 15$ GeV, satisfying shower-shape requirements and matching an ID track [2] [12]. The muon trigger selects muon candidates with $p_{\text{T}} > 13$ GeV and $|\eta| < 2.4$ reconstructed in both the ID and the MS systems and having consistent trajectories [13].

Fully simulated Monte Carlo (MC) event samples are used to develop and validate the analysis procedure, compute detector acceptance and reconstruction efficiency, and aid in the background determination. Samples of events for background processes are generated as described in detail in [14]. For the major backgrounds, Z+jets production and top quark pair production, Alpgen v2.13 [15] and MC@NLO v3.41 [16] interfaced with Herwig [17] are used, respectively. Diboson WW, WZ and ZZ event samples are generated using Herwig, while MadGraph [18] interfaced with Pythia v6.421 [19] is used for $W\gamma$ and $Z\gamma$. Single top-quark production is generated with MC@NLO.

The MC LRSM signal samples were produced using the implementation of this model in Pythia, with Mrst2008LO* modified leading-order parton density functions (PDF) [20], where the W_R gauge boson couples to the opposite chiral components of the SM W-boson. The coupling constants for the W_R and left-handed W-boson are assumed to be the same, including the CKM matrix for W_R coupling to right-handed chiral quark components. It is assumed that there is no mixing between W_R and the SM W-boson. Twenty-four LRSM signal samples were generated for W_R masses ranging from 600 to 1500 GeV and heavy Majorana neutrino masses ranging from 50 to 1300 GeV, with the constraint that $m_N < m_{W_R}$. Similarly to SM neutrinos, heavy Majorana neutrinos can mix if their masses are different. Both the scenarios of no-mixing and 100% mixing between two generations of lepton flavour (e or μ) were considered, assuming that the mass differences between the heavy Majorana neutrinos are very small compared to the experimental resolution on their reconstructed invariant mass. Additionally, for the 100% mixing scenario, it is assumed that there is no mixing between the third lepton generation and the other two.

Both the SS and OS lepton final states were considered. If the heavy neutrinos have a Majorana nature, the new physics signal would contribute to both the SS and OS channels. However, if the heavy neutrinos have a Dirac nature, the new physics signal would contribute solely to the OS final state.

All signal and background samples were produced using the ATLAS underlying event tune [21] and were processed through the ATLAS detector simulation [22] based on Geant4 [23]. The presence of multiple pp collisions within the same bunch crossing, known as "pile-up", can be analysed by examining N_{vtx}, the number of reconstructed primary vertexes in each event. In this data sample, the average value of N_{vtx} was ≈2.3. The MC background samples included a simulation of pile-up and were weighted to match the N_{vtx} distribution observed in data.

[2] The detailed trigger requirements vary throughout the data-taking period, but the thresholds are always low enough to ensure that leptons with $p_{\text{T}} > 20$ GeV lie in the efficiency plateau.

4 Object reconstruction and event selection

Criteria for electron and muon identification closely follow those described in [24]. Electrons are required to pass the "medium" selection criteria, with $p_{\mathrm{T}} > 20$ GeV and $|\eta| < 2.47$, excluding the electromagnetic calorimeter transition region, $1.37 < |\eta| < 1.52$. Electron tracks whose trajectories pass through an active region of the innermost pixel detector are required to have a measurement in that layer in order to suppress electrons from photon conversions. Additionally, an electron whose track matches a muon candidate's ID track is rejected.

Muons are required to be identified either in both the ID and the MS systems (combined muons) or as a match between an extrapolated ID track and one or more segments in the MS. The ID track is required to have at least one pixel hit, more than five SCT hits, and a number of TRT hits that varies with η. For combined muons, a good match between ID and MS tracks is required, and the p_{T} values measured by these two systems must be compatible within the resolution. Only muons with $p_{\mathrm{T}} > 20$ GeV and $|\eta| < 2.4$ are considered. For the final selection, the distance between the z coordinate of the primary vertex and that of the extrapolated muon track at the point of closest approach to the primary vertex must be less than 5 mm while the distance in $r\phi$ must be less than 0.2 mm.

To reduce the background due to leptons from decay of hadrons (including heavy-flavour hadrons) produced in jets, the leptons are required to be isolated. For electrons, the E_{T} deposited in the calorimeter towers in a cone in $\eta - \phi$ space of radius $\Delta R = 0.2$ around the electron position [3] are summed, and the E_{T} of the electron, corrected for energy leakage, is subtracted. An equivalent quantity is calculated for the muon using the same cone size. The energy in this cone is required to be less than 15% of the electron (muon) E_{T} (p_{T}). Additionally, muons within $\Delta R < 0.4$ of a jet with $p_{\mathrm{T}} > 20$ GeV or a candidate electron are rejected.

Jets are reconstructed using the anti-k_{t} jet clustering algorithm [25, 26] with a radius parameter $R = 0.4$. The inputs to this algorithm are clusters of calorimeter cells seeded by cells with energies significantly above the measured noise. Jets are constructed by performing a four-vector sum over these clusters, treating each cluster as an $(E,\vec{p})$ four-vector with zero mass. Jets are corrected for calorimeter non-compensation, upstream material and other effects using p_{T} and η-dependent calibration factors obtained from MC simulation and validated with extensive test-beam and collision-data studies [27]. Only jets with $p_{\mathrm{T}} > 20$ GeV and $|\eta| < 2.8$ are considered. The closest jet to a candidate electron within a distance $\Delta R < 0.5$ is discarded. Events are discarded if they contain any jet failing basic quality selection criteria, which reject detector noise and non-collision backgrounds [28].

Events are required to have at least one reconstructed primary vertex with at least five associated tracks. At least one of the lepton candidates must match a triggered lepton at the last stage of the trigger selection. The preselection signal region is defined as exactly two identified leptons with $p_{\mathrm{T}} > 20$ GeV originating from the primary vertex and at least one jet with $p_{\mathrm{T}} > 20$ GeV. Additionally, to reduce the number of background events from Drell-Yan processes and mis-identified leptons, while keeping sufficient statistics to validate the relevant SM background estimate, the dilepton invariant mass, m_{ll}, is required to be greater than 110 GeV. The signal region is then subdivided into SS and OS dilepton events. Improved sensitivity is achieved with additional optimisation requirements, which are referred to hereafter as the final selection. The W_R invariant mass, m_{lljj}, is required to be greater than 400 GeV. The W_R invariant mass is reconstructed from the leptons and the two highest p_{T} jets in events with at least two jets, or the single jet in events with only one jet, under the assumption that the two jets were reconstructed as one due to their proximity [4]. To further reduce the larger SM background contributions in the OS dilepton channels, the scalar sum of the transverse energies of the leptons and up to the two highest p_{T} jets, denoted by S_{T}, is required to be greater than 400 GeV.

[3] The radius ΔR between the object axis and the edge of the object cone is defined as ($\Delta R = \sqrt{(\Delta\phi)^2 + (\Delta\eta)^2}$.

[4] Anti-k_{t} jets are massive, therefore the jet four-momentum is used in calculating the invariant mass.

5 Background estimation

Several processes have the potential to contaminate the signal regions. The main background to the SS dilepton final state arises from SM W+jets, $t\bar{t} \to lvjjbb$ and QCD multijet production where one or more jets are misidentified as promptly produced isolated leptons [5], which is referred to as "fake lepton" background. This background is determined by a data-driven technique since it cannot be accurately obtained from MC simulation. The other significant backgrounds arise from charge-flip of a reconstructed electron due to a hard bremsstrahlung process in Z+jets and $t\bar{t}$ events. Small contributions from diboson and single top-quark events are also accounted for. For the OS dilepton final state, the dominant backgrounds are Z+jets and $t\bar{t}$ events, with each contributing approximately evenly after all optimisation cuts are applied. Contributions from the fake lepton background, diboson and single top-quark events are also estimated.

A fake lepton originates from either a light-flavour jet mimicking an isolated lepton or a heavy-flavour hadron decaying to produce an isolated lepton. SM processes generating dilepton final states with at least one fake lepton include W+jets, QCD multijets, $t\bar{t}$ and single top-quark production. A data-driven approach, similar to the one described in [8, 14], is used to estimate this background. The method uses "loose" leptons in addition to the candidate leptons. The loose leptons are defined using the same identification selection criteria as the candidate leptons, but with the isolation requirements dropped. The method uses the fractions of these "loose" fake leptons, R_{fake}, and loose prompt leptons, R_{prompt}, which also pass the candidate lepton requirements. A 4×4 matrix is then employed on the "loose-loose" dilepton sample to predict the total fake lepton background to the SS and OS dilepton final states. The R_{fake} ratios are measured from fake lepton enriched control regions with only one loose lepton, and where additional criteria have been imposed to reduce the true lepton contamination from W+jets background to a negligible level. Specifically, the following requirements are imposed: $\Delta\phi(E_{\text{T}}^{miss}, jet \text{ or } e) < 0.1$ for the electron control region and $\Delta\phi(E_{\text{T}}^{miss}, \mu) < 0.5$ for the muon control region, where E_{T}^{miss} is defined as the missing transverse energy based on the calorimeter information and the transverse momenta of muons within $|\eta| < 2.7$ [24]. The R_{prompt} fractions are measured using an unbiased lepton together with a well-identified tag lepton in Z events satisfying $86 < m_{l^{\pm}l^{\mp}} < 96$ GeV. The "tag" lepton is required to satisfy all lepton selection criteria, while the unbiased "probe" lepton should satisfy the loose criteria. To improve the accuracy of the prediction for muons, the ratios are parameterised as a function of kinematic variables. For the electron, a constant fraction R_{fake} is used since no significant variations are observed.

A partially data-driven approach is adopted to estimate $Z \to e^{\pm}e^{\mp}$ and $Z \to \mu^{\pm}\mu^{\mp}$ contributions to the OS dilepton channels. A control region is defined requiring $80 < m_{ll} < 100$ GeV and ≥ 1 jets, where non-Z contributions are found to be negligible. A normalisation factor between the observed data count and the MC prediction is obtained from this region and applied to the MC estimates in the signal region. Those normalisation factors are 0.98 ± 0.02 and 0.97 ± 0.01 for the electron and muon channels respectively. The $e\mu$ contribution is estimated purely from MC simulation due to insufficient $Z \to \tau^{\pm}\tau^{\mp}$ data. The contribution from the fake lepton background is evaluated using the data-driven method described above. All other backgrounds are estimated from MC simulation. To avoid double counting contributions from fake leptons in the MC samples with the data-driven estimate, MC events are required to have two prompt leptons at the truth level. Prior to requiring $m_{ll} > 110$ GeV in the OS $e\mu$ channel, where the sample composition is more representative of the dominant backgrounds in the signal regions, 93 events are observed in data and the total predicted background is 99 ± 4(stat.) $\pm$ 12(sys.), where 67 ± 1(stat.) $\pm$ 10(sys.) originate from $t\bar{t}$, and 18 ± 4(stat.) $\pm$ 7(sys.) from fake lepton background, with additional smaller contributions from Z+jets and diboson.

[5] Prompt particles are particles produced in the hard scattering with a mean lifetime $\tau > 0.3 \times 10^{-10}$s. Therefore, leptons from W, Z and τ are classified as prompt leptons, while leptons from B and D hadron decays are classified as non-prompt leptons.

The fraction of reconstructed electrons with charge-flip due to hard bremsstrahlung via $e^{\pm}_{hard} \rightarrow e^{\pm}_{soft}\gamma_{hard} \rightarrow e^{\pm}_{soft}e^{\pm}_{soft}e^{\mp}_{hard}$, is measured from simulated $Z \rightarrow e^+e^-$ events. The charge of a MC truth electron originating from the Z decay is compared to the reconstructed electron candidate. The fraction is parameterised as a function of the electron E_{T} and η and applied to Z+jets and $t\bar{t} \rightarrow e^{\pm}l^{\mp}b\bar{b}$ MC backgrounds to obtain their contributions to the SS dilepton final state. The data to MC normalisation factor obtained for OS Z events is also applied to extrapolate in the SS sample. The contribution from fake lepton background to the SS final state is estimated using the data-driven method. All other backgrounds are estimated from MC simulation and found to be small. Prior to requiring $m_{ll} > 110$ GeV, the total predicted SM background to the SS dilepton final state for all channels combined is 47 ± 4(stat.) ± 8(sys.) events compared to 43 observed data events, with about equal contributions from the fake lepton background and $Z \rightarrow e^{\pm}e^{\mp}$, where the charge of one of the electrons was flipped.

6 Systematic uncertainties

The dominant source of systematic uncertainties on the SS dilepton channel arises from the uncertainty on the fake lepton background estimate. One component originates from the statistical uncertainty on the parameterization of R_{fake}. This uncertainty is obtained by randomly sampling half of the control region to measure R_{fake} and comparing the predicted with the observed R_{fake} in the second half. A variation up to 30% is observed and propagated to the fake lepton background estimate. To evaluate the magnitude of the uncertainty on the overall fake lepton background estimate, two additional studies have been performed. The former checks the method on simulated data, by comparing the actual background from fake leptons with that predicted by the estimation procedure. The latter uses the region where the sub-leading lepton has a transverse momentum between 10 and 20 GeV. Both studies are consistent with a 30% uncertainty.

The dominant source of uncertainties on the MC background estimates arise from the uncertainties in the jet energy scale [29] and resolution [30] (10% combined), the uncertainty on the electron identification efficiency (6%), and the MC modelling of top pair production and decay (15%). Other uncertainties on lepton energy scale and resolution and lepton triggers are estimated to be $\approx$ 1% each. Uncertainties on LRSM signals due to jet energy scale and resolution are 6% combined while other uncertainties, including variation of the PDFs (7.5%), amount to 10%.

7 Experimental results

The numbers of observed data events and the expected SM background events in the SS and OS final states signal regions for the preselection and final selection are shown in Table 1. Good agreement between the number of data events and the predicted backgrounds is observed. Kinematic distributions of the dilepton-dijet invariant mass and S_{T} in the OS final state for the preselection, hence prior to the additional optimisation criteria on those variables, are compared to the SM expectation in Figure 1 and show good agreement. Figure 2 shows the distribution of m_{lljj}, the reconstructed W_R mass in the SS and OS final states after all the selection criteria have been applied.

Since no excess above the SM background expectation is observed, upper limits on the cross-sections times branching ratios for new physics based on the LRSM models are obtained. Classical confidence intervals in the theoretical cross-section are constructed by generating ensembles of pseudo-experiments that describe expected fluctuations of statistical and systematic uncertainties on both signal and backgrounds, following the likelihood ratio ordering prescription proposed by Feldman and Cousins [31].

The distributions in Figure 2 are used to set the limits in the SS and OS channels on the total production cross-section times branching ratio to $ee, \mu\mu$ for the no-mixing scenario and to $ee, \mu\mu, e\mu$ for the 100% mixing scenario between N_e and N_μ. The limits on the heavy Majorana neutrino and W_R masses,

Table 1: Summary of the expected background yields and observed number of events for the SS and OS dilepton channels. The upper part of the table gives the numbers obtained for the preselection of events with two leptons, ≥ 1 jet and $m_{ll} > 110$ GeV. The lower part of the table gives the numbers for the final selection which additionally requires $M_{W_R} > 400$ GeV and, for the OS channel only, $S_{\mathrm{T}} > 400$ GeV. The first errors are statistical uncertainties and the second are systematic uncertainties excluding the luminosity uncertainty. The uncertainty due to the luminosity is 3.4% for all backgrounds except for the fake lepton(s), which is measured from data.

Physics Processes	SS	OS
	Preselection	
Diboson	$0.18 \pm 0.01 \pm 0.01$	$4.0 \pm 0.1 \pm 0.4$
$t\bar{t}$ + single top	$0.39 \pm 0.01 \pm 0.06$	$56.3 \pm 0.6 \pm 8.0$
$Z \to ll$	$0.81 \pm 0.06 \pm 0.15$	$106.6 \pm 3.2 \pm 14.0$
Fake lepton(s)	$5.81 \pm 1.27 \pm 2.06$	$6.9 \pm 2.3 \pm 2.7$
Total background	$7.2 \pm 1.3 \pm 2.1$	$173.8 \pm 3.9 \pm 16.7$
Observed in data	5	177
	Final selection	
Total background	$1.9 \pm 0.4 \pm 0.5$	$13.3 \pm 1.2 \pm 2.1$
Observed in data	2	10

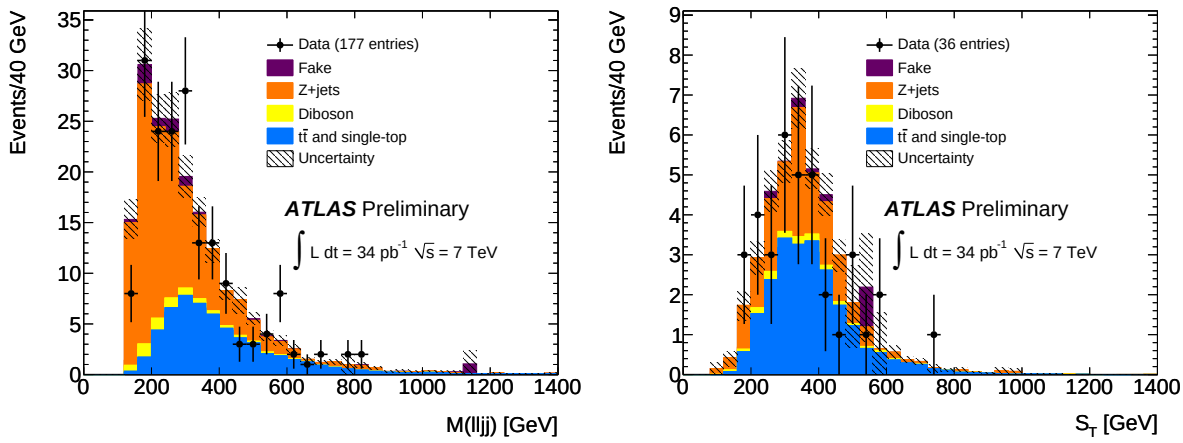

Figure 1: (Left) Distribution of the dilepton-dijet invariant mass, M_{lljj}, for OS dilepton events with ≥ 1 jets and $M_{ll} > 110$ GeV. A selection criterion $M_{lljj} \geq 400$ GeV is used. (Right) Distribution of S_{T} for OS dilepton events with ≥ 1 jets and $M_{ll} > 110$ GeV and $M_{lljj} \geq 400$ GeV. A selection criterion $S_{\mathrm{T}} \geq 400$ GeV is used.

for each mixing scenario, are shown in Figure 3 and determined for SS events and SS+OS events. The SS+OS limit is obtained by combining the two individual limits. Figure 4 shows the excluded cross-section times branching ratio obtained for each mixing scenario. The exclusion region is significantly larger than that obtained previously by other experiments [5, 6, 7], as well as those recently obtained by ATLAS in an inclusive search for SS dilepton signatures [8].

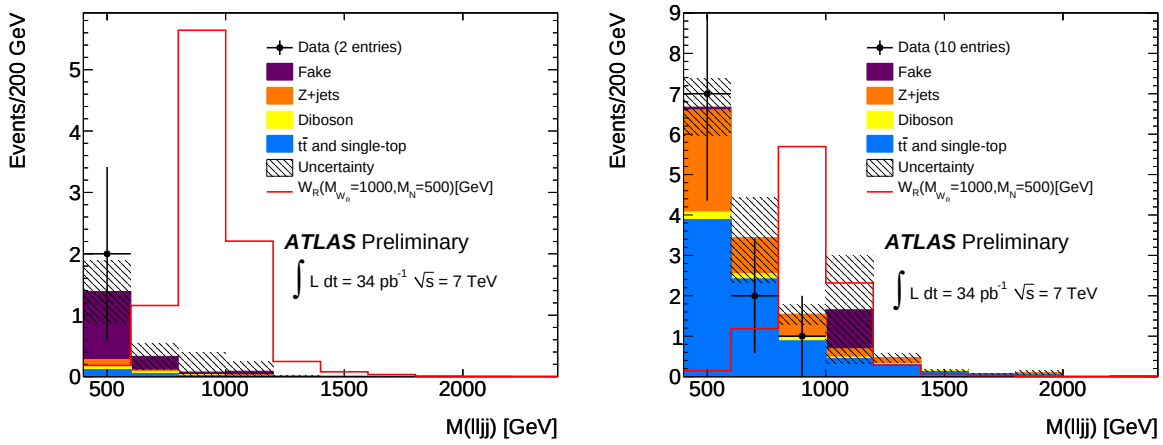

Figure 2: Distribution of the dilepton-dijet invariant mass, M_{lljj}, for SS events (left) and OS events (right) with ≥ 1 jets, $M_{ll} \geq 110$ GeV and $M_{lljj} \geq 400$ GeV. In the OS dilepton events, $S_{\mathrm{T}} \geq 400$ GeV must also be satisfied. The signal distribution for $M_{W_R} = 800$ GeV and $M_N = 300$ GeV is overlaid.

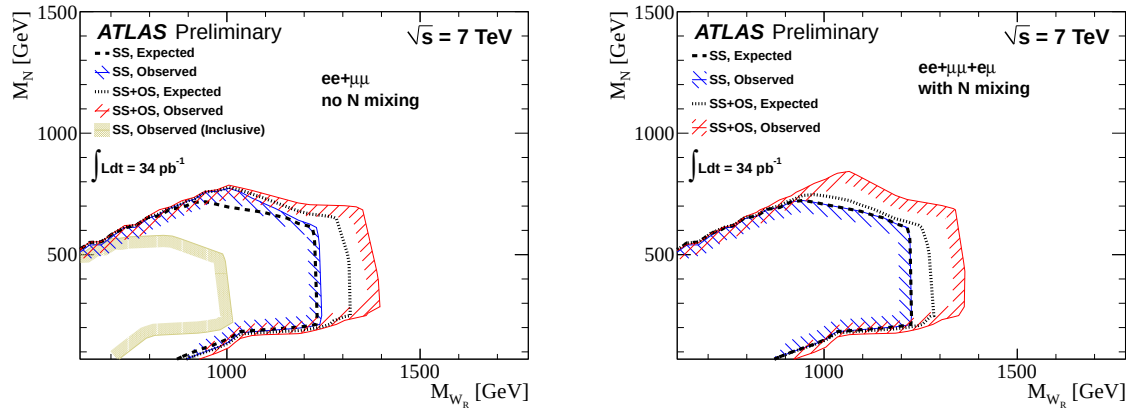

Figure 3: Observed and expected 95% CL upper limits on the heavy Majorana neutrino and W_R masses obtained from the cross-section times branching ratio limits described in the text. The no-mixing scenario is shown on the left, and in the 100% mixing scenario on the right. The excluded region is inside the solid-hatched boundary. The excluded region obtained for SS events in [8] is also shown (labelled "inclusive" in the left plot).

8 Conclusions

In summary, the first dedicated search at the LHC for hypothetical heavy Majorana neutrinos and W_R in final states with two isolated high-p_{T} same-sign or opposite-sign leptons and hadronic jets has been presented. In a data sample corresponding to 34 pb^{-1}, no significant deviations from the SM expectation are observed. Stringent limits are placed on the cross-section times branching ratio for the production of a W_R decaying to heavy Majorana in the context of the Left-Right Symmetric Model. These ATLAS results exceed previous limits set by other experiments [5, 6, 7], as well as those recently obtained by

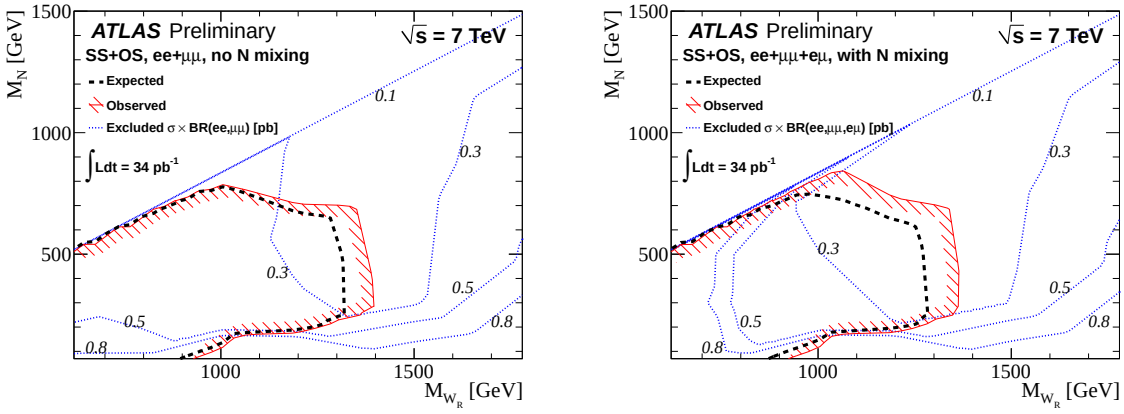

Figure 4: Observed and expected 95% CL upper limits on the heavy Majorana neutrino and W_R masses obtained from the cross-section times branching ratio limits described in the text, for the combined SS+OS channels. The no-mixing scenario is shown on the left, and in the 100% mixing scenario on the right. The exclusion region is the inside solid-hatched boundary. The contours show the observed $\sigma \times BR$ [pb] upper limits as a function of the heavy Majorana neutrino and W_R masses, where σ is the production cross-section of the W_R and BR is the branching ratio to $ee, \mu\mu$ in the no-mixing scenario or $ee, \mu\mu, e\mu$ in the 100% mixing scenario.

ATLAS with a more generic search [8].

References

[1] B. Aharmim et al. (SNO collaboration), Phys. Rev. **C 72** (2005) 055502.

[2] A. Davidson, K. C. Wali, Phys. Rev. Lett. **60** (1987) 18.

[3] R. N. Mohapatra, *Unification and Supersymmetry*. Springer-Verlag, 3rd ed., 2002.

[4] R. N. Mohapatra and P. B. Pal, ISBN 981-238-070-1, *Massive Neutrinos in Physics and Astrophysics*. World Scientific, 3rd ed., 2004.

[5] L3 Collaboration, Phys. Lett. **B 517** (2001) 67–74.

[6] L3 Collaboration, Phys. Lett. **B 295** (1992) 371–382.

[7] V. M. Abazov *et al.* (DØ Collaboration), Phys. Rev. Lett. **100** (2008) 211803.

[8] ATLAS Collaboration, `http://arxiv.org/pdf/1108.0366v1`, Submitted to JHEP (2011) .

[9] ATLAS Collaboration, JINST **3** (2008) S08003.

[10] ATLAS Collaboration, EPJC **71** (2011) 1630.

[11] ATLAS Collaboration, ATLAS-CONF-2011-011 (2011) .

[12] ATLAS Collaboration, ATLAS-CONF-2010-026 (2011) .

[13] ATLAS Collaboration, ATLAS-CONF-2010-095 (2011) .

[14] ATLAS Collaboration, EPJC **71** (2011) 1577.

[15] M. Mangano et al., JHEP **07** (2003) 001.

[16] S. Frixione and B. R. Webber, JHEP **06** (2002) 029; S. Frixione, P. Nason and B. R. Webber, JHEP **08** (2003) 007; S. Frixione, E. Laenen and P. Motylinski, JHEP **03** (2006) 092.

[17] G. Marchesini, B. R. Webber, G. Abbiendi et al., Comput. Phys. Commun. 67, 465-508 (1992); G. Corcella, I. G. Knowles, G. Marchesini et al., JHEP 0101, 010 (2001); G. Corcella et al., HERWIG 6.5 release note, CERN-TH/2002-270 (2005) [hep-ph/0210213v2].

[18] J. Alwall, P. Demin, S. de Visscher et al., JHEP (2007) 0709:028.

[19] T. Sjostrand et al., *PYTHIA v6.4.21*, JHEP **05** (2006) 026.

[20] A. Sherstnev and R. S. Thorne, Eur. Phys. J. **C 55** (2008) 553.

[21] ATLAS Collaboration, ATL-PHYS-PUB-2010-002 (2010) .

[22] ATLAS Collaboration, Eur. Phys. J. **C 70** (2010) 823.

[23] S. Agostinelli et al., (GEANT4 Collaboration), Nucl. Instr. Meth. **A506** (2003) 250.

[24] ATLAS Collaboration, JHEP **12** (2010) 060.

[25] M. Cacciari and G. P. Salam, Phys. Lett. **B 641** (2006) 57.

[26] M. Cacciari, G. P. Salam and G. Soyez, `http://fastjet.fr/`.

[27] ATLAS Collaboration, ATLAS-CONF-2010-050 (2010); E. Abat et al., Nucl. Instr. Meth. A621 (2010) 134.

[28] ATLAS Collaboration, ATLAS-CONF-2010-099 (2010) .

[29] ATLAS Collaboration, Eur. Phys. J. **C 71** (2011) 1512.

[30] ATLAS Collaboration, ATLAS-CONF-2010-054 (2010) .

[31] G. J. Feldman, R. D. Cousins, Phys. Rev. **D 57** (1998) 3873.

A Appendix: Candidates event displays

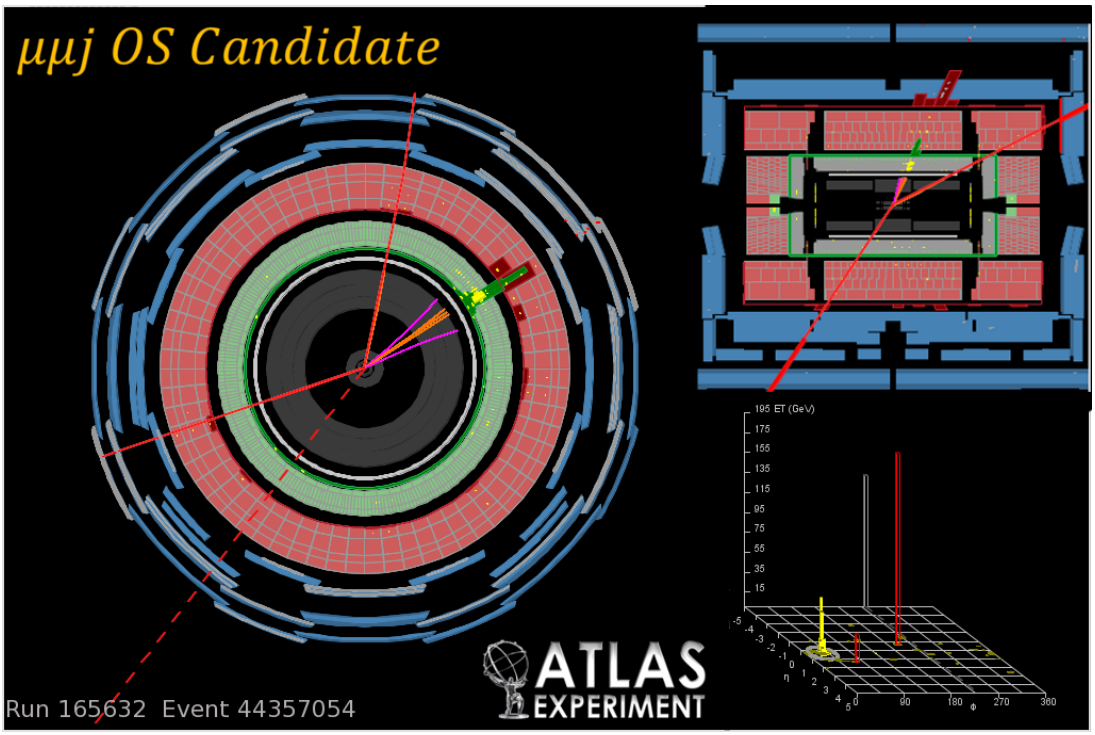

Figure 5: Event display of the highest M_{lljj} event in the OS dimuon channel. The highest momentum muon has a p_T of 192 GeV and an (η, ϕ) of $(-0.62, -2.81)$. The subleading muon has a p_T of 28 GeV and an (η, ϕ) of $(0.43, 0.59)$. The jet has p_T of 288 GeV and an (η, ϕ) of $(0.40, 0.57)$. The dimuon invariant mass is 218 GeV, $M_{lljj} = 586$ GeV and $S_T = 509$ GeV.

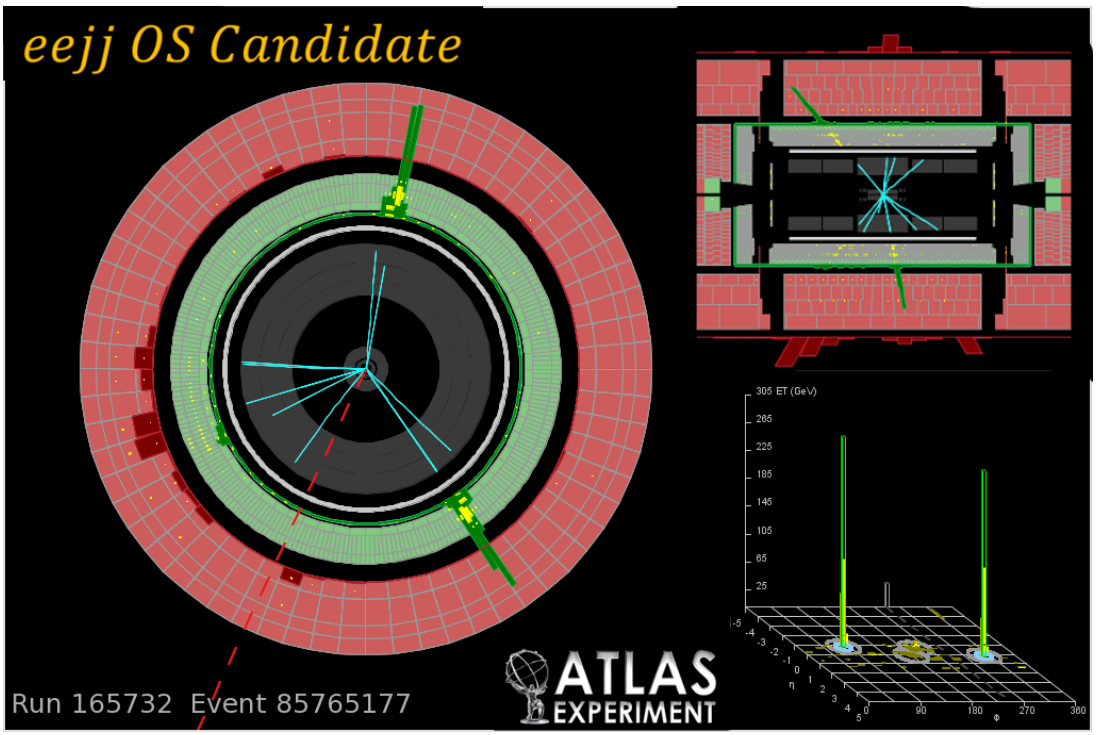

Figure 6: Event display of the highest M_{lljj} event in the OS dielectron channel. The highest energy electron has an E_T of 301 GeV and an (η, ϕ) of $(-0.78, 1.40)$. The subleading electron has an E_T of 266 GeV and an (η, ϕ) of $(0.18, -0.96)$. The highest energy jet has p_T of 118 GeV and an (η, ϕ) of $(-0.66, -2.74)$. The subleading jet has p_T of 50 GeV and an (η, ϕ) of $(0.14, 3.12)$. The dielectron invariant mass is 696 GeV, $M_{lljj} = 815$ GeV and $S_T = 739$ GeV.

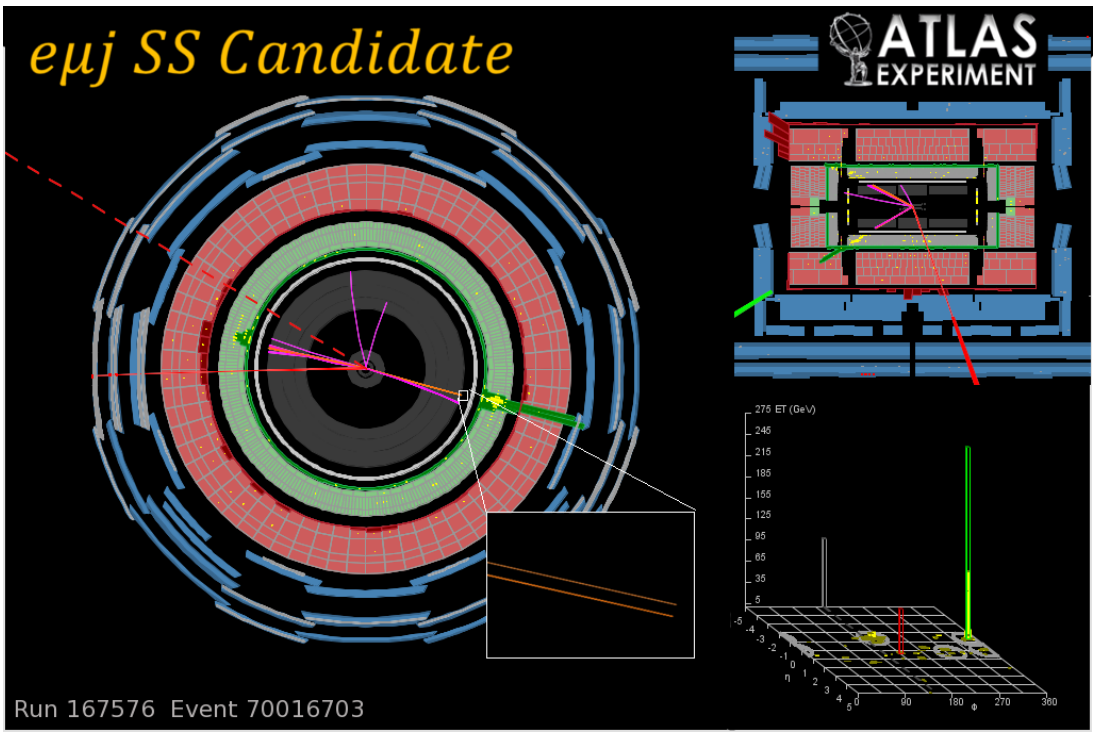

Figure 7: Event display of a SS dilepton candidate. The electron has an E_T of 273 GeV and an (η, ϕ) of $(-1.28, 0.28)$. The presence of a close-by track near the electron track makes it a good candidate for a charge-flip reconstructed electron due to a hard bremsstrahlung. The subleading muon has a p_T of 63 GeV and an (η, ϕ) of $(0.36, 3.12)$. The jet has p_T of 159 GeV and an (η, ϕ) of $(-1.39, 2.88)$. The dilepton invariant mass is 353 GeV and M_{lljj} = 582 GeV.